Synthesis of Magnesium Silicate Hydrate as an Adsorbent for Different Dyes

PASINEE PANITH[1], WORAWAT WATTANATHANA[1], WANCHAI DEELOED[2], RATTHAPIT WUTTISARN[1], SUTTIPONG WANNAPAIBOON[3], YURANAN HANLUMYUANG[1], NOLLAPAN NOOTSUWAN[1], CHATCHAI VERANITISAGUL[4] and APIRAT LAOBUTHEE[1]*

[1]Department of Materials Engineering, Faculty of Engineering, Kasetsart University, Ladyao, Chatuchak, Bangkok 10900, Thailand.
[2]Department of Chemistry, Faculty of Science, Kasetsart University, Ladyao, Chatuchak, Bangkok 10900, Thailand.
[3]Synchrotron Light Research Institute, 111 University Avenue, Suranaree, Muang, Nakhon Ratchasima 30000, Thailand.
[4]Department of Materials and Metallurgical Engineering, Faculty of Engineering, Rajamangala University of Technology Thanyaburi, Pathumthani 12110, Thailand.
*Corresponding author E-mail: fengapl@ku.ac.th

ABSTRACT

Magnesium silicate hydrate was synthesized for using as an adsorbent for different commercial organic dyes. X-ray diffraction (XRD) confirmed the crystalline phase of magnesium silicate hydrate. Some characteristic absorption bands of the magnesium silicate hydrate structure were observed in the Fourier transform infrared spectroscopy (FTIR) spectrum which supported the result identified from XRD data. Analysis of surface area and porosity by surface area analyzer showed that the synthesized magnesium silicate had high surface area of 634.63 m^2/g and also showed the average BJH pore size of 3.72 nm. Insight into the sorption isotherm curve, the hysteresis characteristic was clearly observed suggesting a presence of mesopores within the obtained material. Dye adsorption study revealed that the synthesized adsorbent had the strongest affinity to the cationic dye (methylene blue) on account of the negative charge on the surface of the adsorbent. Hence, the adsorption of methylene blue was reached the equilibrium at the fastest time. In all, the results showed a possibility to apply this prepared magnesium silicate materials as a selective adsorbent for cationic dyes.

Keywords: Magnesium silicate, Hydrothermal synthesis, Adsorbent, Dyes.

INTRODUCTION

Dyes are usually applied to materials to provide desired colors. They are widely employed in different industries e.g., pharmaceutical, food, cosmetics, plastics, photographic, paper industries, among others[1]. Dyes can be adhered to a variety of surfaces ascribed to the formation of covalent

bonds, coordination complexes with certain metal ions, or even via physical adsorption like Van der Waals (VdW) attractions[2]. There are many types of dyes which can be categorized by their applications and/or different chemical structures. The key feature within organic dyes attributed to their intense colors is the group of atoms called chromophores. These chromophore centers consist of diverse functional groups, such as azo (-N=N-), anthraquinone, methine (-CH-), nitro (-NO$_2$), carbonyl (-CO-), and others. In addition, there are electrons withdrawing or donating substituents so-called auxochromes, which generate and/or intensify the color of the chromophores. Among those, amine, carboxyl, sulfonate, and hydroxyl groups are the most common-used functional groups[3].

It is known that many thousand dyes and pigments are widely used in industry, and hence several tons of synthetic dyes are annually produced worldwide[4]. In addition, the heightened demand for textile products increases the demand of synthetic dyes production. The immensive proportional use of synthetic dyes and inefficient dyeing process contribute to the dye wastewater, which nowadays becomes one of the crucial sources of severe pollutions[5]. At the end of dyeing cycles, used dye substances are typically led to be passed through a wastewater treatment and later be released to the natural environments, i.e. commonly into canals and rivers. Due to their chemical inertness in the ambient condition as well as their high stability to light, the used dyes vastly remain as chemical pollutants within the eco-systems[6]. For instance, in case of the "Reactive Blue 19" dye, it requires about 46 years to let half of the amounts to be biodegraded via hydrolysis at pH 7 and 25°C[7]. Based on this circumstance, most of dyes and pigments are strategically designed to be resistant for biodegradation in order to extend their utilization-lifetime in products. Hence, investigation of effective methods to remove dye residues in nature is of concern.

Recently, the conventional methods of dye removal from contaminated water involve several processes, such as flocculation[8], ozonation[9], membrane filtration[10] and photocatalytic and biological degradation[11]. Among these treatments, adsorption process is considered as one of the most efficient routes owing to its relatively low-cost, simple deployment, and short operation period[12-14]. In

details, the dye adsorption can be broken down into several steps; (i) the dye molecules first encounter the boundary layer between the adsorbent and the adsorbate; (ii) then they diffuse from the boundary film onto adsorbent surface; (iii) finally they diffuse into the porous structure of the adsorbent. Certain adsorbing materials have been investigated to remove synthetic dyes from the wastewater such as activated carbon[15-16], hydroxides[17-20], inorganic clays [21-23], among others. Because of its non-toxicity, low cost, superior adsorption capacity, fast adsorption rate and high availability, magnesium silicate had become one of the most interesting adsorbent materials[24]. In this paper, we examined the affinity of the synthesized magnesium silicate towards the adsorption characteristics of some cationic and anionic dyes. The detailed characterizations are thoroughly explained hereafter and indicate herein the potential use of magnesium silicate for dye removal.

EXPERIMENTAL

Materials preparation

The starting materials, magnesium nitrate hexahydrate (Mg(NO$_3$)$_2$.6H$_2$O) was received from Merck & Co. while sodium silicate (Na$_2$SiO$_3$) was supplied from TIAN-NAM Chemical Industrial Trade. Propylene glycol–400 was a commercial-grade product proving by Suksapanpanit, Thailand. Magnesium silicate powders were prepared by a hydrothermal method. Na$_2$SiO$_3$, with the volume of 0.9 mL was dissolved in water, while 1.48 g of Mg(NO$_3$)$_2$.6H$_2$O was dissolved in the mixture of propylene glycol–400 and ethanol with the volume ratio of 3 to 1. After the two solutions were mixed, a white precipitate was formed. The pH of this step was kept at the value of 10. The obtained mixture was transferred into an autoclave and treated at 150°C for 24 hours. The hydrothermally treated products were further filtered and washed with distilled water several times until the pH of the washing solution was at 7. The obtained product was then dried at 80°C overnight prior to material characterizations and adsorption study.

Materials Characterization

Powder X-ray diffraction (XRD) was performed at ambient temperature at Beamline1.1W (Multiple X-ray Techniques) at Synchrotron Light Research Institute, Thailand using the

monochromatic synchrotron X-ray radiation of the energy 8046 eV (wavelength of 1.5409 Å, equally to Cu Kα radiation). The powder sample was packed in Kapton capillary with a diameter of 0.5 mm and aligned using goniometer head. It should be noted that the capillary was constantly rotated during the powder XRD measurement. The diffraction pattern was recorded by a strip detector (Mythen6K 450, Dectris®) in the 2θ range of 10-90°. Fourier transform infrared spectrophotometer (Bruker Alpha) was used to reveal chemical functional groups in the prepared magnesium silicate powder before the dye adsorption process. The sample was thoroughly grounded with KBr and uniaxially pressed into a pellet and then used for the measurement in transmission mode. All peaks in the range 4000 - 400 cm^{-1} were recorded with a spectral resolution of 2 cm^{-1}. The morphology study was done under a scanning electron microscope (SEM, FEI Quanta 450). The sample was preliminarily sputter-coated with gold to avoid charging problem. Nitrogen adsorption-desorption measurements were carried out using a Micromeritics 3Flex surface area and porosity analyzer. The samples were degassed at 200°C for 24 h prior to the nitrogen gas adsorption measurement. The specific surface area (SBET) of the prepared powder was calculated in accordance with the BET (Brunauer-Emmett-Teller) principle referring to the nitrogen adsorption isotherm at 77 K. Moreover, full adsorption and desorption isotherms were also recorded.

Dye adsorption study

The weight of the prepared magnesium adsorbent was 0.1 g for all experiments. The dyes used in this work were methylene blue (MB), reactive blue 19 (RB19), and methyl orange (MO). MB is a cationic dye while RB19 and MO are anionic dyes[25]. The concentrations of MB, RB19 and MO used in the whole experiments were fixed at 50 ppm. The adsorbent was added to the 20 cm^3 of solutions of each dye, and then the mixtures were shaken for 6 hours. Samplings of the reaction mixture were regularly uptaken out every 60 min in order to measure their absorbance at λ_{max} by using an ultraviolet-visible spectrometer (Shimadzu PhamaSpec 1700 model). The sampling solutions were centrifugated prior to the UV-Vis absorption study.

The quantity adsorbed was calculated by the following equation:

$$q_e = [(C_0-C_f)V]/1000W,$$

Where q_e is the amount of dye adsorbed by the adsorbent in mg g^{-1}. C_0 and C_f are initial and final concentration in mg dm^{-3} in the solution, V and W represent the volume of solution (dm^{-3}) and weight of the adsorbent (g), respectively. The effect of pH on the MB adsorption was also examined by adjusting the pH of the solutions to 5, 6, 7, 8 and 9 using 1 M HCl hydrochloric acid or 1 M sodium hydroxide. Moreover, the adsorption characteristic was studied with a variety of the adsorbent contents, namely 0.01 g, 0.05 g and 0.10 g. However, the concentration of the MB dye was used 100 ppm instead of 50 ppm in these studies to emphasize the effects of pH and the adsorbent contents on MB adsorption characteristics.

RESULTS AND DISCUSSION

Material Characterization

The diffraction pattern of the solid magnesium silicate prepared from hydrothermal method is shown in (Fig. 1 A). It was observed that the diffraction peaks were corresponding to the crystalline phase of magnesium silicate hydrate (2MgO.3SiO$_2$.2H$_2$O) rather than those of non-hydrated MgSiO$_3$ phase. Although the degree of crystallinity of the hydrated product is relatively low (mainly due to the lack of the final calcination step), this result indicated the successful synthesis of magnesium silicate hydrate. A key imperative to having the hydrated form is to avoid the agglomeration of particles, which could later lead to a poor performance for dye adsorption. Fourier transform infrared (FTIR) spectrum of the obtained magnesium silicate hydrate is displayed in (Fig. 1 B). The broad peak around 3450 cm^{-1} was attributed to the O-H stretching vibration[26-27] of the moisture adsorbed on the surface of the magnesium silicate hydrate and/or the water of crystallization in the crystal structure of magnesium silicate hydrate. There is an absorption around 1640 cm^{-1} corresponding to O-H bending vibration and confirming the presence of O-H stretching peak as discussed previously[28-29]. Characteristic peak of magnesium silicate structure (Si-O-Si symmetrical stretching vibration) was found at 1016 cm^{-1} [30]. Moreover, the bands at 662 and 462 cm^{-1} were arisen from Si-O bending and Mg-O vibration, respectively[30]. The scanning electron microscopic (SEM) image of the prepared magnesium silicate hydrate is illustrated in (Fig. 1 C). Evidently, it was observed that the microstructure of the prepared magnesium silicate was plate-like particles due

to the preferred spatial growth of the magnesium silicate hydrate particles during the hydrothermal crystallization. The size distribution of magnesium silicate hydrate sheet is depicted in (Fig. 1 D). The mean thickness was found to be 42 ± 9 nm. Full nitrogen adsorption isotherms of the sample are shown in (Fig. 2 A) while BJH pore size distribution from

desorption isotherm is portrayed in (Fig. 2 B). The isotherms suggested a mesoporous characteristic as the hysteresis loop was clearly observed due to the different pathways of N_2 adsorption and desorption after the monolayer adsorption. In addition, the mesopores were presented within the material with an average size of 3.7 nm according to the BJH analysis.
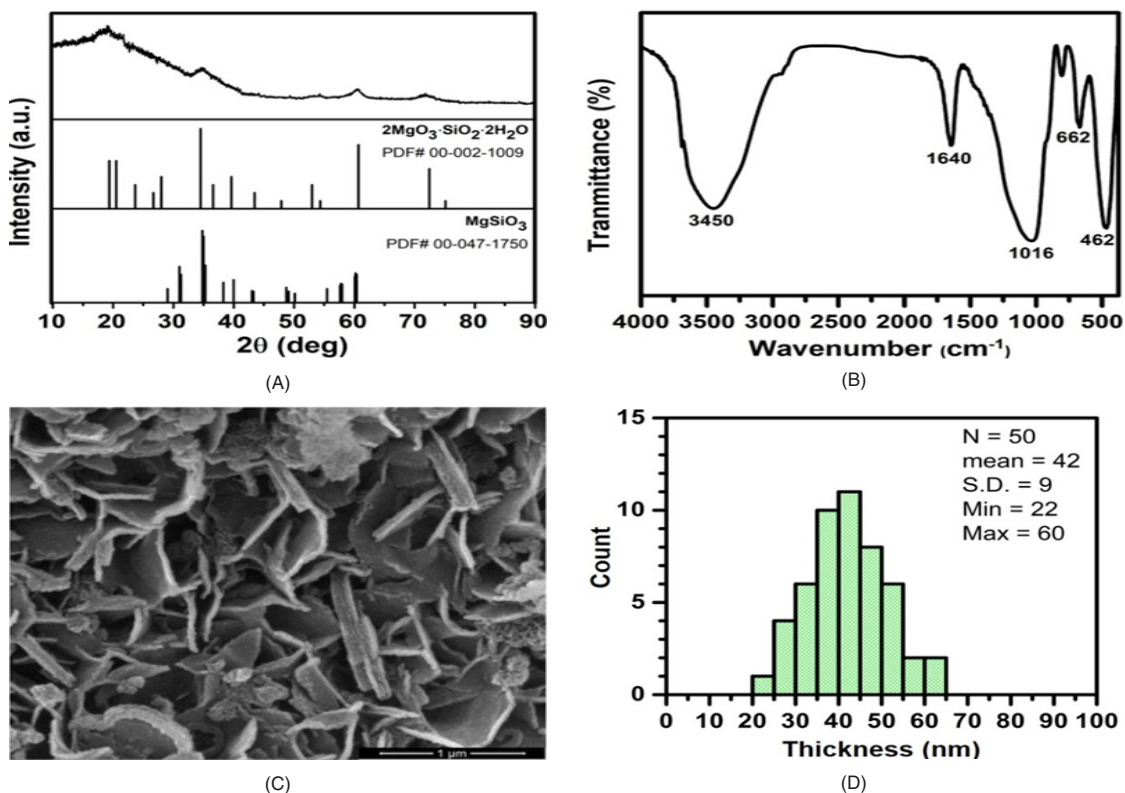

(A)

(B)

(C)

(D)

Fig. 1. Material Characterization; (A) X-ray diffraction of the synthesized magnesium silicate hydrate from hydrothermal method compared to the standard compounds with JCPDS cards of 00-002-1009 and 00-047-1750; (B) FTIR spectrum of synthesized magnesium silicate hydrate; (C) SEM image of the synthesized magnesium silicate; and D) The thickness distribution of the particles of magnesium silicate hydrate
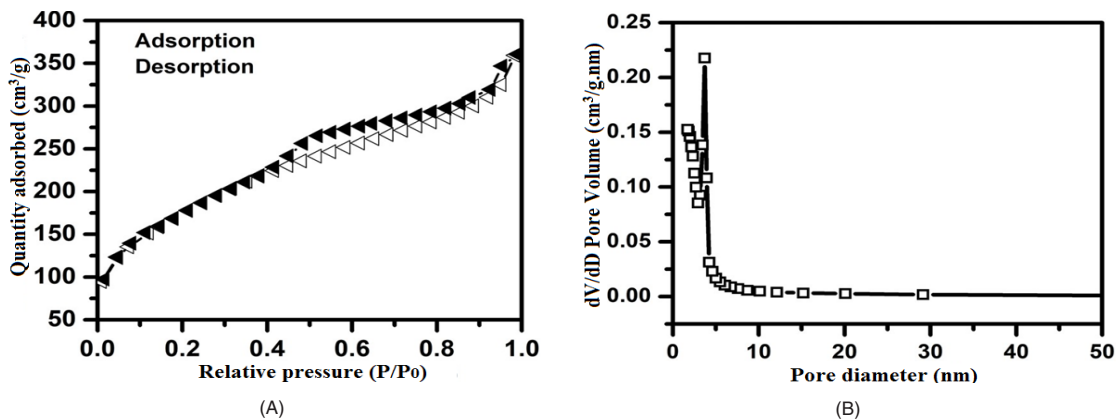

(A)

(B)

Fig. 2 (A). Full adsorption and desorption nitrogen isotherms at 77 K and (B) its corresponding BJH pore size distribution of the prepared magnesium silicate hydrate

Dye adsorption study

On the study of dye adsorption capacity and selectivity, the magnesium silicate hydrate was submerged into the aqueous solutions of the dyes, decisively chosen for their structural characteristics, i.e. charges (cationic and anionic dyes), and molecular weights (Fig. 3 A). The adsorption capacity of the synthesized adsorbent, herein magnesium silicate hydrate, for the tested dyes was ranged from lowest to highest as following: MO, RB19, and MB. The highest adsorption in the case of MB could be attributed to the compact molecular size of MB (1.7 nm X 0.76 nm)[31], making it easier to diffuse into the pores of the magnesium silicate, of which the average pore size is 3.72 nm. Moreover, the other possible factor for excellent adsorption may be originated from the electrostatic attraction between negatively charged surface of the adsorbent and the positive charge on the nitrogen atom within the MB dye. On the contrary, the lower adsorption capacity of other dyes (RB19 and MO (1.2 nm[32])) can be explain in part by the electrostatic repulsion between the negative charge on the anionic dyes and the negative charge on the surface of the adsorbent. Also seen from the figure, the adsorption of MB took only 30 min in order to achieve the saturated adsorption ca. 18.1, while the equilibrated times for the remaining two dyes were longer than 1 hour. Moreover, lower saturated adsorptions were observed for these two dyes.

The pH of the solution is also an important attribute controlling the adsorption process. The results in (Fig. 3 B) show that the adsorption of MB on magnesium silicate hydrate increases from the value of 6.32 mg/g to 7.61 mg/g when reducing the pH of the solutions from 9 to 5. The maximum adsorption quantity was found at the pH of 5 (7.61 mg/g) which was in agreement with the previous work reported by Hazzaa, R. and Hussein, M (2014)[33]. At lower pH, the surface charge may get more positive, according to the dye protonation process by H+ ions in the solution. Consequently, this promotes the stronger adsorption of the dye on the negatively-charged surface of the adsorbent than the ones at higher pH. For the effect of the adsorbent dosages on the adsorption rate of MB, it was observed that the rate of MB adsorption was less than 15 min to reach the saturation quantity. As the content of the adsorbents decreased, the rate of equilibrium attainment also decreased

(Fig. 3 C). This was because of the more available active sites of the adsorbate. All aforementioned arguments reveal that magnesium silicate hydrate is a promising candidate for the selective adsorption of cationic dyes like methylene blue.
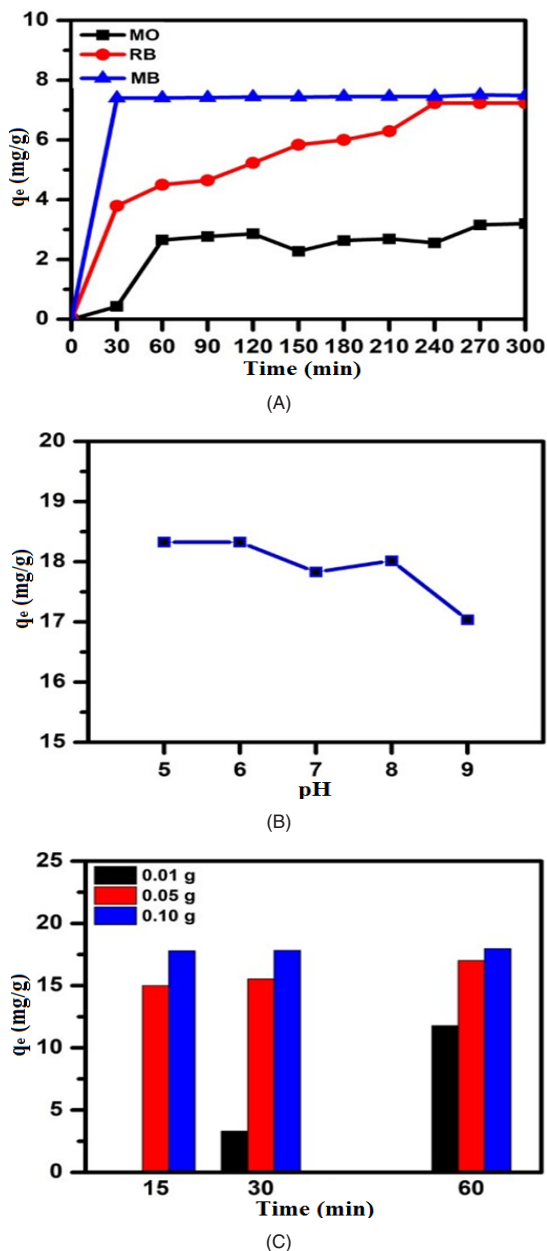

(A)

(B)

(C)

Fig. 3 (A) Adsorption quantities of different dyes as a function of time; (B) Adsorption quantity of methylene blue as a function of pH of the dye's solution; (C) Adsorption quantity of methylene blue as a function of adsorbent content. Note that the concentrations of all dyes used in (A) were 50 ppm while the concentration of the MB dye used in (B) and (C) were 100 ppm

CONCLUSION

Magnesium silicate hydrate was synthesized by hydrothermal crystallization for using as an adsorbent for commercial organic dyes. The crystalline phase of the prepared adsorbent was identified to be magnesium silicate hydrate by synchrotron-based powder X-ray diffraction (XRD). In addition, characteristic peaks, e.g. O-H peaks (stretching and bending) and Si-O-Si vibration observed in the Fourier transform infrared spectroscopy (FTIR) spectrum of the synthesized adsorbent confirmed the result from XRD. The synthesized magnesium silicate was found to have high BET surface area with the value of 634.63 m^2/g and the average BJH pore size was 3.72 nm. According to nitrogen sorption isotherm, it revealed that there were also mesopores within the synthesized magnesium silicate hydrate which was consequently suitable for dye adsorption. From the dye adsorption study, the synthesized adsorbent showed the strongest capacity to the cationic dye (methylene blue) as a result from the electrostatic attraction between its negatively charged surface and the positively charged dye molecules. Moreover, the adsorption of methylene blue was also reached the equilibrium at the shortest time interval among the other tested dyes. These results showed a possibility for the prepared magnesium silicate hydrate to be used as a selective adsorbent for cationic dyes.

Conflict of interest
There is no conflict of interest to declare.

REFERENCES

1. Carneiro, P.A.; Nogueira, R.F.P.; Zanoni, M.V.B. *Dyes Pigm.*, **2006**, *74*(1), 127-132. doi: 10.1016/j.dyepig.2006.01.022.

2. Bafana, A.; Devi, S.S.; Chakrabarti, T. *Environ Rev.*, **2011**, *19*(1), 350-370. doi:10.1139/a11-018.

3. dos Santos, A.B.; Cervantes, F.J.; van Lier, J. B. *Bioresour Technol.*, **2007**, *98*(12), 2369-2385. doi: 10.1016/j.biortech.2006.11.013.

4. Nandhini, N.T.; Rajeshkumar, S.; Mythili, S. *Biocatal Agric Biotechnol.*, **2019**, *19*, 101138. doi:10.1016/j.bcab.2019.101138.

5. Ogugbue, C.J.; Sawidis, T. *Biotechnol Res Int.*, **2011**, 967925. doi:10.4061/2011/967925.

6. Rodríguez Couto, S. *Biotechnol Adv.* **2009**, *27*(3), 227-235. doi:10.1016/j.biotechadv. 2008.12.001.

7. Firmino, P.I.M.; da Silva, M.E.R.; Cervantes, F.J.; dos Santos, A. B. *Bioresour Technol.,* **2010**, *101*(20), 7773-7779. doi:10.1016/j. biortech.2010.05.050.

8. Ma, J.; Wang, R.; Wang, X.; Zhang, H.; Zhu, B.; Lian, L.; Lou, D. *J. Environ. Chem. Eng.*, **2019**, *7*(3), 103049. doi:10.1016/j. jece.2019.103049.

9. Zhu, C.; Farah, J.; Choël, M.; Gosselin, S.; Baroudi, M.; Petitprez, D.; Visez, N. *Environ Pollut.*, **2018**, *242*, 880-886. doi:10.1016/j. envpol.2018.07.025

10. Khumalo, N.P.; Vilakati, G.D.; Mhlanga, S.D.; Kuvarega, A.T.; Mamba, B.B.; Li, J.; Dlamini, D.S. *J. Water Process Eng.*, **2019**, *31*, 00878. doi:10.1016/j.jwpe.2019.100878.

11. Waghmode, T.R.; Kurade, M.B.; Sapkal, R.T.; Bhosale, C.H.; Jeon, B.-H.; Govindwar, S.P. *J. Hazard. Mater.*, **2019**, 115-122. doi:10.1016/j. jhazmat.2019.03.004.

12. Chaari, I.; Fakhfakh, E.; Medhioub, M.; Jamoussi, F. *J. Mol. Struct.*, **2019**, *1179*, 672-677. doi:10.1016/j.molstruc.2018.11.039.

13. Kurtan, U.; Amir, M.; Yildiz, A.; Baykal, A. *Appl. Surf. Sci.*, **2016**, *376*, 16-25. doi: 10.1016/j. apsusc.2016.02.120

14. Mohebali, S.; Bastani, D.; Shayesteh, H. *J. Mol. Struct.*, **2019**, *1176*, 181-193. doi: 10.1016/j.molstruc.2018.08.068.

15. Auta, M.; Hameed, B.H. *Chem. Eng. J.*, **2011**, *175*(1), 233-243. doi:10.1016/j.cej. 2011.09.100.

16. Tan, I.A.W.; Ahmad, A.L.; Hameed, B.H. *J. Hazard. Mater.*, **2008**, *154*(1-3), 337-346. doi: 10.1016/j.jhazmat.2007.10.031.

17. Shamsayei, M.; Yamini, Y.; Asiabi, H. *J. Colloid Interface Sci.*, **2018**, *529*, 255-264. doi:10.1016/j.jcis.2018.06.022.

18. Ling, F.; Fang, L.; Lu, Y.; Gao, J.; Wu, F.; Zhou, M.; Hu, B. *Microporous and Mesoporous Mater.*, **2016**, *234*, 230-238. doi:10.1016/j.micromeso.2016.07.015.

19. Ruan, X.; Chen, Y.; Chen, H.; Qian, G.; Frost, R.L. *Chem. Eng. J.*, **2016**, *297*, 295-303. doi:0.1016/j.cej.2016.01.041.

20. Liu, S.; Li, B.; Qi, P.; Yu, W.; Zhao, J.; Liu, Y. *Colloids Interface Sci. Commun.*, **2019**, *28*, 34-40. doi:10.1016/j.colcom.2018.11.004.

21. Borisover, M.; Davis, J.A. *Developments in Clay Science.*, **2015**, *6*, 33-70. doi: 10.1016/B978-0-08-100027-4.00002-4.

22. Xu, R; Mao, J.; Peng, N.; Luo, X.; Chang, C. *Carbohydr. Polym.*, **2018**, *188*, 143-150. doi:10.1016/j.carbpol.2018.01.073.

23. Bentahar, S.; Dbik, A.; Khomri, M.E.; El Messaoudi, N.; Lacherai, A. *Groundwater for Sustainable Development.*, **2018**, *6*, 255-262. doi:10.1016/j.gsd.2018.02.002.

24. Zhang, J.; Dang, L.; Zhang, M.; Lu, Q.; Zhao, S. *Surf. Interfaces.*, **2017**, *8*, 112-118. doi:10.1016/j.surfin.2017.05.005.

25. Qiu, J.; Feng, Y.; Zhang, X.; Jia, M.; Yao, J. *J. Colloid Interface Sci.*, **2017**, *499*,151-158.

26. Wattanathana, W.; Veranitisagul, C.; Wannapaiboon, S.; Klysubun, W.; Koonsaeng, N.; Laobuthee, A. *Ceram. Int.*, **2017**, *43*(13), 9823-9830. doi: 10.1016/j.ceramint. 2017. 04. 162.

27. Nantharak, W., Wattanathana, W., Klysubun, W., Rimpongpisarn, T., Veranitisagul, C., Koonsaeng, N., Laobuthee, A. *J. Alloys Compd.*, **2017**, *701*, 1019-1026. doi:10.1016/j.jallcom.2017.01.090.

28. Veranitisagul, C.;Wattanathana,W.;Nantharak, W.; Jantaratana, P.; Laobuthee, A.; Koonsaeng, N. *Mater. Chem. Phys.*, **2016**, *177*, 48-55. doi: 10.1016/j.matchemphys.2016.03.038.

29. Wattanathana, W.; Nootsuwan, N.; Veranitisagul, C.; Koonsaeng, N.; Suramitr, S.; Laobuthee, A. *J. Mol. Struct.*, **2016**, *1109*, 201-208. doi: 10.1016/j.molstruc.2015.12.069.

30. Rashid, I.; Daraghmeh, N.H.; Al Omari, M.M.; Chowdhry, B.Z.; Leharne, S.A.; Hodali, H.A.; Badwan, A.A. *Profiles Drug Subst Excip Relat Methodol.*, **2011**, *36*, 241-285. doi: 10.1016/B978-0-12-387667-6.00007-5.

31. Li, L.; Liu, X.L.; Gao, M.; Hong, W.; Liu, G.Z.; Fan, L.; Hu, B.; Xia, Q.H.; Liu, L.; Song, G.W.; Xu, Z.S. *J. Mater. Chem.* A., **2014**, *2*(6), 1795-1801. doi: 10.1039/c3ta14225.

32. Wu, Q.-Y.; Liang, H.-Q.; Li, M.; Liu, B.-T.; Xu, Z.-K. *Chinese J Polym Sci*. (English Edition)., **2016**, *34*(1), 23-33. doi:10.1007/s10118-016-1723-6.

33. Hazzaa, R.; Hussein, M. *Environmental Technology & Innovation.*, **2015**, *4*, 36-51. doi: 10.1016/j.eti.2015.04.002.